Journal of Advanced Engineering Trends
ISSN : 2682 - 2091

Vol. 44, No. 1, January 2025

Performance enhancement of DCT-and DHT-based OFDM Systems over Doubly Dispersive Fading Channels

Gerges M. Salama[1,*], Mai M. S. Ezz-Eldin[2], Sherif A. Elshawadfy[1]
[1] *Electrical Engineering Dep., Faculty of Engineering, Minia University, Minia, Egypt*
[2] *Electrical and Communication Engineering Dep., Future High Institute of Engineering, Fayoum, Egypt*
[*]*Corresponding Author: Email: gerges.salama@mu.edu.eg*

ARTICLE INFO
Article history:
Received: 13 September 2024
Accepted: 9 January 2025
Online: 26 February 2025

Keywords:
Discrete DCT, DHT, OFDM, PAPR, SLM, PTS

ABSTRACT
This research proposes the use of Discrete Cosine Transform (DCT) and Discrete Hartley Transform (DHT) within Orthogonal Frequency Division Multiplexing (OFDM) systems to improve the performance of the conventional Discrete Fourier Transform (DFT) in OFDM systems. The examination of Bit Error Rate (BER) performance and the mitigation of Peak-to-Average Power Ratio (PAPR) in various OFDM systems over a doubly dispersive fading channel is presented. This work initially examines the attributes of DFT-, DCT-, and DHT-based OFDM systems, then employs signal processing algorithms to mitigate PAPR through the Selected Mapping (SLM) and Partial Transmit Sequence (PTS) techniques. Mathematical verification confirms that these methods will improve BER performance and decrease PAPR. The simulation results indicate that employing DCT- and DHT-based OFDM systems, as opposed to DFT-based OFDM systems, improves the BER performance by 4 dB, achieving a BER of 10^{-3}. The proposed reduction plan for PAPR thresholds is statistically viable. Statistically, a large enhancement in PAPR mitigates nonlinear oscillations in OFDM systems.

1. Introduction

In cellular mobile channels, multipath effects, time-varying rapid fading, and Doppler frequency shifts cause fading and inter-symbol interference (ISI) in the receiver signal. These phenomena result in reception errors and decreased communication performance. OFDM systems, extensively employed in high-rate transmission systems such as mobile networks, HIPERLAN Type II, IEEE 802.11, IEEE 802.16, and digital video broadcasting (DVB), surpass single-carrier systems in environments characterized by multipath fading [1].

The substantial implementation difficulty of OFDM is partly due to the transmitted signal's high PAPR and wide dynamic signal range with an extraordinarily high PAPR [2]. At the transmitter end, a nonlinear power amplifier causes the OFDM signal to be clipped. Clipping causes spectral spread and reduces Bit Error Rate (BER) performance [3,4]. One approach to resolve this issue is to guarantee that the amplifier functions inside its linear domain. Unfortunately, such a remedy is not efficient and successful. Power efficiency is essential for wireless communications because it allows for small-size terminals, reduces power consumption, and offers enough coverage across a large region. As a result, it's critical to ensure the power amplifier runs well with low back-off settings and to attempt to prevent signal clipping. Before transmission, not many changes can be made to the OFDM signal. Consequently, it has become an important research topic to develop a computationally effective algorithm to minimize PAPR in OFDM systems [3].

Many ideas have been proposed and reviewed in the literature to achieve the above objective. For example, we consider filtering clipping, block coding, and selected mapping in addition to tone reservation (TR) optimization [5,6]. The majority of these methods, meanwhile, frequently employ the OFDM sub-carrier symbols since there is a relationship of sorts between them. Hence, the PAPR reduction achieved by both methods is equal and comes at the cost of a more complex OFDM transceiver, a high coding overhead, and/or the need for a certain kind of authenticating transmitter/receiver signal.

This work investigates methods to reduce the PAPR of OFDM transmissions utilizing the DCT. PAPR reduction is achieved by leveraging DCT's ability to concentrate energy in specific frequency bins. The OFDM data is modulated using DCT and then the Inverse Fast Fourier Transform (IFFT) reduces significantly the PAPR. DCT-OFDM, as opposed to SLM-OFDM and PTS-OFDM, maintains the orthogonality of the system without adding noise or necessitating further data transmission. DCT-OFDM is a viable strategy for PAPR reduction in OFDM systems since it minimizes PAPR effectively and has minimal hardware complexity.

Similarly, DHT was used instead of the DFT-OFDM, and improved accuracy was recorded for superior performance and dispersive selective channels [7].

This work suggests developing a DCT-based OFDM system as a substitute for the conventional DFT-OFDM system, one that can function over doubly dispersive fading channels. The system's performance is assessed for a range of Doppler shifts. Furthermore, a performance comparison is made between the DHT-based OFDM system and the traditional DFT-based OFDM system, as well as the DCT-based OFDM system.

DCT-based OFDM systems have tremendous potential in a wide range of applications due to their ability to minimize intercarrier interference (ICI) and improve spectral efficiency. DCT-based OFDM systems generally operate in the following areas:

1. Wireless Communication: DCT-based OFDM systems find applications in wireless communication systems like Wi-Fi, LTE,

and 5G. Their superior performance in bit error rate (BER) and peak-to-average power ratio (PAPR) renders them suitable for high-speed data transmission.

2. Cognitive Radio Networks: The two systems, collectively and independently, can enhance spectrum efficiency. The DCT-based approach streamlines spectrum detection and facilitates the identification of available channels.

3. Underwater Acoustic Communication: DCT-based OFDM systems are appropriate for underwater acoustic communication, characterized by extremely fluctuating channel circumstances. The resilience of DCT against multipath fading and Doppler shifts renders it an optimal selection for dependable data transmission in underwater settings.

4. Power Line Communication (PLC): DCT-based OFDM is an ideal alternative to PLCs since it increases data transmission speeds while decreasing interference and noise in power line situations.

5. Satellite Communication: We use DCT-based OFDM to enhance the efficiency of data flow. They are well-suited for use in satellite communication systems due to their low inter-carrier interference and high spectrum efficiency.

The structure of this document is as follows: The DFT-based OFDM system is covered in Section II, and the DCT-based OFDM system is described in Section III. Section V covers the properties of doubly dispersive fading channels, whereas Section IV presents the DHT-based OFDM system. In Section VI, the suggested schemes' performance is analyzed and simulation experiments are presented. Section VII provides a conclusion to the paper.

2. DFT-based OFDM System

A. The Discrete Fourier Transform (DFT)

By representing samples of the Discrete-Time Fourier Transform (DTFT) at equally spaced frequencies, the DFT converts a finite series of uniformly spaced samples into a similar sequence of the same duration. Because of its effectiveness and applicability for Fourier analysis, the DFT is a key instrument in signal processing that is utilized extensively.

A sequence of N complex numbers are altered via DFT $\{x_n\} = x_0, x_1, x_2, \dots \dots x_{N-1}$ into a different series of complex numbers $\{X_n\} = X_0, X_1, X_2, \dots \dots X_{N-1}$, Which is defined as:

$$X_k = \sum_{n=0}^{N-1} x_n . e^{\frac{-2\pi}{N} kn}$$

$$= \sum_{n=0}^{N-1} x_n . \left[\cos\left(\frac{2\pi}{N}\, kn\right) - i\,.\ \sin\left(\frac{2\pi}{N}\, kn\right)\right] \qquad (1)$$

where k retrieves integer numbers from $\{0, \dots, N\}$.

B. The OFDM System

Several restricted-band subchannels that transmit simultaneously to accomplish high data rate transmission while prolonging the signal length to eliminate ISI are created by the multicarrier modulation technique known as OFDM. To stop different broadcasts from interfering with one another and to shield the OFDM system from inter-carrier interference (ICI), which is brought on by the spread of channel delay, cyclic prefixes (CP) or guard intervals (GI) are essential. Fig. 1 displays the typical block diagram of an OFDM system based on DFT.

The complex symbols $\{s_{n,k}\}_{k=0}^{N-1}$ with variance $E|s_{n,k}|^2 = \sigma_s^2$, Which is transmitted at the n^{th} OFDM block, subsequently, the OFDM modulated signal can be represented as:

$$S_n(t) = \sum_{k=0}^{N-1} s_{n,k}\ e^{-j2\pi k\Delta f t} \quad , 0 \le t \le T_s \qquad (2)$$

where T_s represents the duration of the sign, Δf Denotes the subchannel spacing, and N is the sub-channel number in OFDM. The receiver's symbol period must be sufficient to modulate the OFDM signal like $T_s \Delta f$=1, which is referred to the condition of the orthogonal, ensuring that $e^{-j2\pi k\Delta f t}$ remains orthogonal for different values of k. In the absence of the duration of the channel, the orthogonality of the transmitted symbols $S_{n,k}$ can be expressed at the receiver as illustrated in equation (3)

$$S_{n,k} = \frac{1}{T_s} \int_0^{T_s} s_n(t)\ e^{-j2\pi k\Delta f t}\ dt \qquad (3)$$

Equation (2) can be used to express the sampled form of the sampled baseband. $S_n(t)$ of the OFDM signal

$$s_n(m\tfrac{T_s}{N}) = \sum_{k=0}^{N-1} s_{n,k}\ e^{-j2\pi k\Delta f m\frac{T_s}{N}}$$

$$= \sum_{k=0}^{N-1} s_{n,k}\ e^{-j2\pi\frac{mk}{N}}, \quad t = m\frac{T_s}{N} \qquad (4)$$

where m is the sample index.

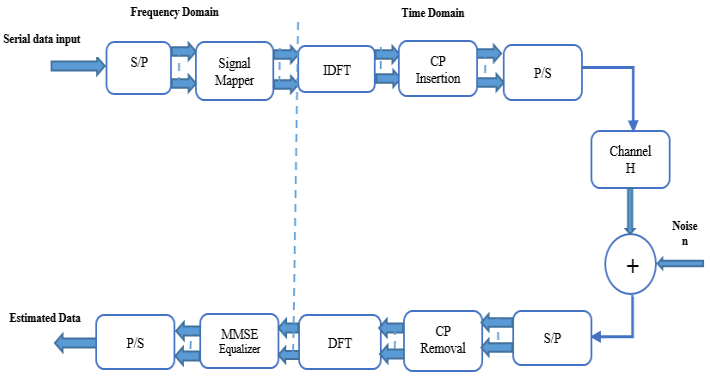

Figure 1: DFT-based OFDM system block diagram

The transmitted symbol of the Inverse Discrete Fourier Transform (IDFT) $\{s_{n,k}\}_{k=0}^{N-1}$ is illustrated in Equation (4). Therefore, it is simple to show that DFT rather than integral in equation (3) can be used to carry out the demodulation procedure.

A cyclic prefix (CP) is necessary to protect an OFDM system against Inter-Carrier Interference (ICI) caused by the delay spread of distant channels. Typically, the CP is positioned between two OFDM blocks. If the channel delay spread is greater than or equal

to the channel CP length, Inter-Symbol Interference (ISI) is eliminated [8]. The duration of an OFDM symbol when there is no CP is T_s . However, with the CP, the transmission time extends to $T = T_g + T_s$. Equation (5) illustrates the OFDM symbol:

$$\tilde{s_n} = \sum_{k=0}^{N-1} s_{n,k}\, e^{-j2\pi k\Delta f t} \quad , \quad -T_g \le t \le T_s \qquad (5)$$

3. DCT-based OFDM System

Like DFT, DCT is a Fourier-related transform that is limited to real numbers. The entire cosine function, which oscillates at various frequencies, is expressed by DCT [9].

As shown in Figure 2, we created a standard scheme DCT-based OFDM system in this research. The suggested approach substitutes a DCT block for the DFT block in the receiver route, making it comparable to the DCT-based OFDM system.

Similarly, the IDFT block is replaced by an IDCT block in the transmission route. The important orthogonal co-sinusoidal functions that make up the DCT-based OFDM system are as follows [9]: $\varphi_n = \cos(2\pi f_n t)$, where $0 \le t < T$, *and* $n = 0, 1, \cdots, N-1$. The minimum subcarrier spacing in a DFT-based OFDM system with real-valued signals can be reduced from $\left(\frac{1}{T}\right)$ Hz to $\left(\frac{1}{2T}\right)$ Hz by utilizing co-sinusoidal orthogonal functions $cos\left(\frac{2\pi nt}{2T}\right)$. The DCT-OFDM signal baseband is defined as:

$$x(t) = \sum_{n=0}^{N-1} X_n \cos\left(\frac{\pi nt}{2T}\right) \qquad n = 0, \ldots, N-1 \qquad (6)$$

The suggested system can be modulated and demodulated using the DCT and IDCT, respectively. Equation (7) defines the representation of discrete-time for this system.

$$x(k) = \sqrt{\frac{2}{N}} \sum_{n=0}^{N-1} X_n B_n \cos\left(\frac{\pi n(2k+1)}{2N}\right) \qquad k=0,\ldots, N-1 \qquad (7)$$

where

$$B_n = \begin{cases} \sqrt{\frac{1}{2}}, & n = 0 \\ 1, & k = 1, \ldots, N-1 \end{cases} \qquad (8)$$

Furthermore, the comparable signal in the frequency domain is provided by equation (9):

$$X_{DCT}(n) = \sqrt{\frac{2}{N}} \sum_{n=0}^{N-1} x_{DCT}(k) B_k \cos\left(\frac{\pi n(2k+1)}{2N}\right),$$

$n = 0, \ldots, N-1$ (9)

Equation (10) illustrates IDCT representation:

$$X_{IDCT}(n) = \frac{2}{N-1} \sqrt{\frac{2}{N}} \sum_{n=0}^{N-1} x_{DCT}(k) B_k \cos\left(\frac{\pi n(2k+1)}{2N}\right) \qquad (10)$$

The benefits of the DCT-based OFDM system are as follows [10]:

1- Energy concentration and spectral compaction are two of the DCT foundation's best features.
2- Due to the offset frequency having less ICI power leakage to nearby subcarriers than OFDM, it is less resilient to offset frequency.
3- By utilizing real arithmetic, DCT considerably lowers the complexity and power requirements of DFT signal processing.

One of the primary limitations of DCT-based OFDM is its inability to directly process complicated signals due to its dependence on real arithmetic. Symmetric guard sequences and pre-filter designs are necessary at the receiver to manage the channel's impulse response, ensuring diagonalization and adequate filtering.

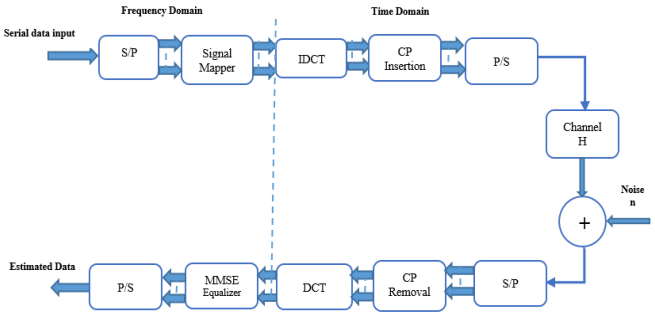

Figure 2: DCT-based OFDM system block diagram

4. DHT-based OFDM System

Akin to Fourier transform, one essential transformation is the Hartley transform which transfers real-valued functions back to real-valued functions without requiring complex values [4]. The Hartley transform of a function $f(t)$ is defined as follows:

$$\boldsymbol{X}_{DHT}(\omega) = \frac{1}{\sqrt{2\pi}} \int_0^{T_s} f(t) cas(\omega t) dt \qquad (11)$$

where

$$cas(t) = cos(t) + sin(t) = \sqrt{2} cos\left(t - \frac{\pi}{4}\right) = \sqrt{2}\sin\left(t + \frac{\pi}{4}\right)$$

The representation of the angular frequency is ω. The Hartley transform is unique in that it may be used as its inverse. This means that the DHT of a real sequence $d = [d_0\ d_1\ \ldots d_{N-1}]^T$ stays consistent because the transformation formula is the same for both the DHT and its inverse (IDHT), and equation (12) illustrates its inverse as follows:

$$\boldsymbol{x}_n = \sum_{k=0}^{N-1} d_k\, cas\left(\frac{2\pi kn}{N}\right), \quad 0 \le n \le N-1$$
$$\boldsymbol{d}_k = \sum_{n=0}^{N-1} x_n\, cas\left(\frac{2\pi kn}{N}\right), \quad 0 \le k \le N-1 \qquad (12)$$

The DHT's real orthogonal matrix is defined using sine and cosine matrix representations [12]. The (n, m) entries of the $N \times N$ matrices C and S are defined in equation (13):

$$\boldsymbol{C}(m,n) = cos\left(\frac{2\pi nm}{2N}\right), \quad 0 \le n, m$$
$$\boldsymbol{S}(m,n) = sin\left(\frac{2\pi nm}{2N}\right), \quad 0 \le N-1 \qquad (13)$$

The IDHT matrix can be represented as shown in equation (14).

$$\boldsymbol{X}_{IDHT} = \frac{1}{\sqrt{N}}(\boldsymbol{C} + \boldsymbol{S}) \tag{14}$$

Proving this is straightforward $\boldsymbol{X}_{DHT}\boldsymbol{X}_{IDHT} = \boldsymbol{I}_N$.

With the same adjustments as the DCT-based OFDM system, the suggested DHT-based OFDM design is comparable to the DFT-based OFDM architecture, as shown in Figure 3. The primary difference lies in using DHT instead of IDFT at the transmitter and DFT instead of DHT at the receiver. This approach offers the advantage of using identical DHT hardware for both the transmitter and receiver in the OFDM system.

While the DHT is less computationally demanding than the DFT and has the same form as its inverse (IDHT), using DHT-based OFDM in wireless communications presents two major obstacles.

Firstly, PAM and BPSK are examples of one-dimensional (1D) modulation techniques that are necessary because the DHT is a real-valued transformation. Secondly, DHT-OFDM is unable to diagonalize the multipath directly channel impulse response (CIR) because of the intrinsic characteristics of the DHT [11,12].

Although it creates a more complex system, the authors of [12] suggested a DHT-based OFDM system that uses a technique to diagonalize the fading channel's equivalent matrix, enabling the use of 2-D modulation schemes like QPSK. Furthermore, situations resembling the DCT-based OFDM system that involve doubly selective channel fading require a complex equalizer.

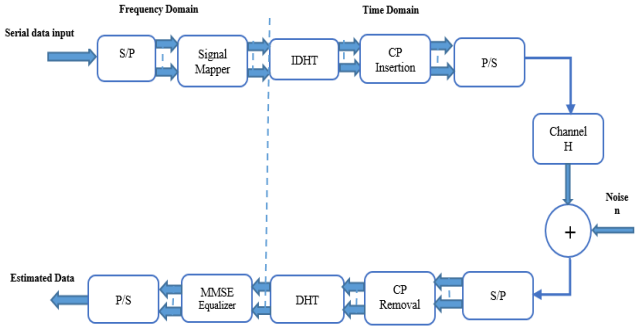

Figure 3: DHT-based OFDM system block diagram

5. Doubly Dispersive Channel

A time-varying channel is produced in radio transmission applications when movement between the receiver and transmitter modifies the propagation path. The growing pace of these conditions leads to rapid fading.

Several variables affect multipath effects, including the existence of reflecting objects in a propagation environment that is always changing. While some wave energy is dispersed by reflection and dispersion, other times it reaches the receiver unhindered in a direct line of sight (LOS). Each multipath component travels a varied distance, and variations in the phase and amplitude of multipath components add to signal strength variations.

Small-scale fading and Rician fading, which occur in highways and small villages, have an envelope amplitude that follows a Rician distribution when the received signal has numerous reflected beams and a strong line-of-sight component. As the amplitude decreases to zero, the Rician Probability Density Function (PDF) approaches the Rayleigh PDF [13]. Put differently, fading statistics on a small scale are described by the Rayleigh distribution when the line-of-sight path is obstructed, while they follow a Rician distribution when it is present.

The symbols are obtained as follows if block-by-block processing is taken into account within the block for a linear time-invariant (LTI) frequency-selective noisy channel:

$$r_n = H_n\, F^* s_n + n_g \tag{15}$$

where r_n is received sequence, H_n is the $N\,X\,N$ channel matrix, F the matrix of DFT/DCT/DHT, F^* is matrix of IDFT/IDCT/DHT, s_n is the data of the transmitted, and n_g is the time-domain Additive White Gaussian Noise (AWGN). Function (16) generates the received vector $\hat{r_n}$ following DFT/DCT/DHT demodulation.

$$\hat{r_n} = F\, H_n\, F^* s_n + F\, n_g \tag{16}$$

Because of the cyclic prefix, H_n becomes a circulant matrix under stationary conditions, enabling the DFT/DCT/DHT matrix to decouple. By adjusting the received sequence's phase and amplitude, the received signal is effectively equalized thus, FH_nF^* is a diagonal matrix [14]. In [15], a single-carrier FDM system has multiple overlapping but orthogonal narrowband subchannels inside its wideband spectrum, enabling the effective conversion of a frequency-selective channel into nearly non-frequency-selective sub-channels via the OFDM system. When frequency fading occurs within the specified bandwidth, each subchannel's frequency response can be broadly characterized as constant. Therefore, a straightforward single-tap equalizer can be utilized to compensate for the multi-path fading channel. Furthermore, OFDM systems are strengthened by the application of a cyclic prefix, which replicates the final segment of an OFDM symbol.

Fast-fading remote channels sometimes involve time-frequency-selective (dispersive) channels, rendering conventional methods inefficient and requiring an intricate equalization for the OFDM system [17]. The speed at which the transmitter and/or receiver move can affect channel fading, leading to Doppler shifts in the components of the received signal. These Doppler shifts often cause the fading response to vary in the presence of a doubly dispersive fading channel. Function (17) illustrates the calculations of the Doppler shift as follows:

$$f_d = \left(\frac{\Delta v}{c}\right) f_c \tag{17}$$

where f_c is the signal carrier frequency, c is the light speed, Δv is the velocity difference between the transmitter and the receiver, and f_d is the Doppler shift frequency.

In the frequency domain, the channel matrix H_n illustrates in equation (15) is neither constant nor diagonal across successive OFDM blocks in a Linear Time-Varying (LTV) channel. Because of this, the useable channel components and inter-carrier interference (ICI) differ from block to block.

6. PAPR Problem

The high Peak-to-Average Power Ratio (PAPR) of the transmitted OFDM signal is one of the primary disadvantages. When this potent PAPR signal passes via a nonlinear apparatus, like a transmitter for a power amplifier, it results in considerable out-of-band radiation and in-band distortions. Bit error rate (BER) is increased by out-of-band radiation, and in-band distortion is the cause of unacceptable interference between adjacent channels [12]. Transmitter power consumption efficiency is quite low when no PAPR reduction measures are used.

The combined OFDM signals can occasionally show high peak power because each subcarrier of the OFDM signal is modified individually. This peak power tends to increase with a higher number of subcarriers. PAPR is commonly used to quantify peak power. Equation (18) defines the PAPR of the transmitted OFDM signal as:

$$PAPR = \frac{\max_{0\le t\le NT} |s(t)|^2}{1/NT \int_0^{NT} |s(t)|^2 dt} = \frac{\max_{0\le n\le N-1} |s_n|^2}{E[|s_n|^2]} \quad (18)$$

The denominator indicates the average signal power, whereas the numerator represents the instantaneous maximum power. The PAPR's complementary cumulative distribution function (CCDF), which shows the likelihood that a data block's PAPR will rise above a specific threshold γ., i.e., $P_r(PAPR > \gamma)$, is used to assess a multi-carrier system's PAPR performance.

In [12], provides a simple approximation of the CCDF of the PAPR of a multicarrier signal. The central limit theorem states that for a multicarrier signal with many subcarriers, the imaginary and real components of the time-domain signal samples with Nyquist rate sampling have zero mean and 0.5 variances, respectively, and follows Gaussian distributions. As a result, the multicarrier signal's amplitude displays a Rayleigh distribution, while its power distribution has two degrees of freedom and is centered around a chi-square distribution:

$$F(\gamma) = 1 - exp(\gamma) \quad (19)$$

Assuming that there is no correlation between the samples, the probability that the PAPR falls below a given threshold level γ that utilized to find the CCDF for the peak power of each OFDM symbol:

$$P(PAPR > \gamma) = 1 - P(PAPR \le \gamma) \quad (20)$$

$$P(PAPR > \gamma) = 1 - F(\gamma)^N \quad (21)$$

Substituting (20) in (21):

$$P(PAPR > \gamma) = 1 - (1 - exp(-\gamma))^N \quad (22)$$

A. *The Selected Mapping Technique (SLM)*

The transmitter generates many candidate data blocks identical to the original data block using the Selected Mapping (SLM) technique, thereafter selecting the one with the lowest PAPR for transmission. Fig. 4 shows the block diagram for the SLM technique. U-phase sequences, whose length is equal to the data block, are multiplied by each data block.

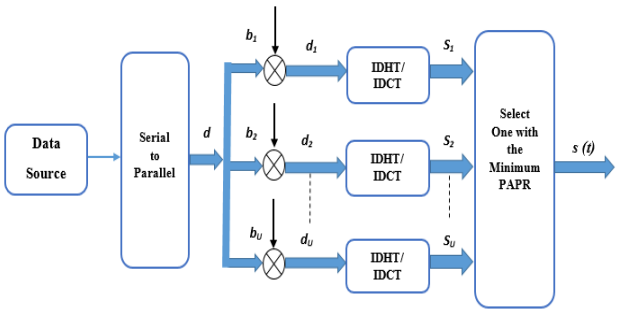

Figure 4: A block diagram of the SLM technique

$$\boldsymbol{B}_u = \left[\boldsymbol{b}_{u,0}, \boldsymbol{b}_{u,1}, \dots, \boldsymbol{b}_{u,N-1}\right]^T, \quad u = 1, 2, \dots, U \quad (23)$$

U adapted data blocks resulting. b1 is all set to include in our search the original data block. The $\boldsymbol{u}^{th}$ candidate vector produced by multiplying the phase vector data block is indicated as $\boldsymbol{d}_u$, so we can write the equation to get the k^{th} element of u^{th} candidate vector as:

$$\boldsymbol{d}_{u,k} = d_k \boldsymbol{B}_{u,k} \quad , u = 1, 2, \dots, U \quad (24)$$

For the $\boldsymbol{u}^{th}$ phase sequence, the adapted data block is:

$$\boldsymbol{d}_u = \left[\boldsymbol{d}_0 \boldsymbol{b}_{u,0}, d_1 \boldsymbol{b}_{u,1}, \dots, d_{N-1}\, \boldsymbol{b}_{u,N-1}\right]^T, u = 1, 2, \dots, U \quad (25)$$

the multicarrier signal $\boldsymbol{s}_u$ can be obtained from equation (26), after applying SLM to $\boldsymbol{d}$

$$\boldsymbol{s}_u = \boldsymbol{F}_{-\alpha}.\boldsymbol{d}_u \quad (26)$$

The transmission of the data block with the lowest PAPR was chosen. To ensure accurate recovery of the transmitted signals, the receiver must be informed about the selected independent vectors. These sequences should be sent as side information to the receiver. For every data block, the SLM approach necessitates $(log_2 U)$ side information bits in addition to additional $U - 1$ transformation operations. This method works with any number of subcarriers and any kind of modulation.

The following equation can be used to quantify the likelihood that $PAPR_{min}$ exceeds γ by choosing the frame with the lowest PAPR from U statistically independent OFDM frames that contain the same information:

$$P(PAPR_{min} > \gamma) = (P(PAPR > \gamma))^U \quad (27)$$

$$P(PAPR_{min} > \gamma) = (1 - (1 - exp(-\gamma))^N)^U \quad (28)$$

From (28), the PAPR reduction amount for SLM depends on the number of phase sequences U and the phase sequence design. All data blocks can reduce PAPR, but their efficiency can vary from one to another.

B. *The Partial Transmit Sequence Technique*

Discontinuous sub-blocks or clusters are generated from the input data block by the application of the Partial Transmit Sequence (PTS) technology. The subcarriers within each sub-block are weighted using a carefully selected phase factor to lower the PAPR of the total signal. Generally, three partitioning methods are employed: partitions that are neighboring, pseudo-random, and interleaved.

The PTS technique block diagram is shown in the Fig.5. K disjoint sub-blocks are created from the input data block d, where K is an integer number; each block contains N/K nonzero elements and N-(N/K) zeros (complete each one by zero padding), so the kth sub-block is given by:

$$\boldsymbol{d}_k = \left[0, \dots, 0, \boldsymbol{d}_{(k-1)(N/K)}, \dots, \boldsymbol{d}_{k(N/K)-1}, 0, \dots, 0\right]^T \quad (29)$$

where $\boldsymbol{d}_k$ is N element vector and $\boldsymbol{d} = \sum_{k=1}^{K} \boldsymbol{d}_k$, $k = 1, 2, \dots, K$ the time domain signal $\boldsymbol{s}_k$is obtained after each of the portioned signals $\boldsymbol{d}_k$ is transformed, we refer to these time-domain signals as partial transmit sequences. In the set denoted by $\boldsymbol{b} = [\boldsymbol{b}_1, \boldsymbol{b}_2, \dots, \boldsymbol{b}_K]^T$, these PTSs are mixed with different complex phase factors.

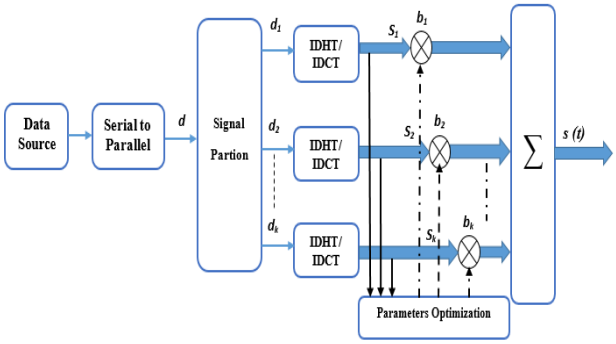

Figure 5: A block diagram of the PTS technique

The key task is to find the set of PAPR-minimizing phase factors. Equation (30) defines a finite number of elements, limiting the difficulty in determining the optimal phase factors.

$$\boldsymbol{P} = e^{j2\pi l/w} \quad , \qquad l = 0,1, \dots, w - 1 \qquad (30)$$

where w is the number of phase factors allowed. It is obvious that with the number of sub-blocks K, The search complexity increases exponentially.

The receiver needs to understand the process used to generate the phase factors and the transmitted signal applied to rotate the subcarriers accordingly. The redundancy brought about by the PAPR reduction strategy for PTS is reflected in the number of bits required for this side information. It is important to note that the PTS technique requires fewer redundancy bits than the SLM technique.

The reduction in PAPR is influenced by the number of phase factors w and the number of sub-blocks K. Additionally, the method of sub-block partitioning can impact the effectiveness of PAPR reduction in the PTS technique. PTS applies to any number of subcarriers and supports all modulation schemes

7. Simulation and Results

The suggested systems are illustrated in this section using the IEEE 802.11a standard system. The channel estimate findings can be used to assess the diagonalized channel characteristics of the DHT-based OFDM and DCT-based OFDM systems. As per the IEEE 802.11a standard, the number of subcarriers utilized is $N_a = 96$, $N = 128$, $l = 8$. Here, N represents the number of subcarriers, l denotes the CP data, and $\Delta f = 20\ MHz$ is involved. An exponential power delay profile with a root-mean-square delay of $\sigma = 3$ were used to simulate the double Rayleigh fading channels.

Table 1: Simulation Parameters

FFT size, N	**128**
Number of subcarriers, N_a	**96**
FFT sampling frequency, Δf	**20 MHz**
Doppler shift frequency, f_d	**75 Hz**
Modulation schemes	**QPSK**

7.1. Comparison between DFT-, DCT-, and DHT-based OFDM systems performance at the same Doppler shift

The BER performance of the DFT-, DCT-, and DHT-based OFDM systems was evaluated using a Doppler shift frequency of parameter $f_d = 75\ Hz$. As illustrated in Fig. 7, both the DCT- and DHT-based OFDM systems outperform the DFT-based OFDM system. Specifically, at the same Doppler shift of $f_d = 75\ Hz$, the conventional DFT-based OFDM system requires an E_b/N_0 of approximately 3 dB to achieve the same BER (10^{-3}) that the DCT- and DHT-based OFDM systems achieve.

Furthermore, identical to the Doppler shift, the DCT-based OFDM system's BER performance is marginally superior to the DHT-based OFDM systems.

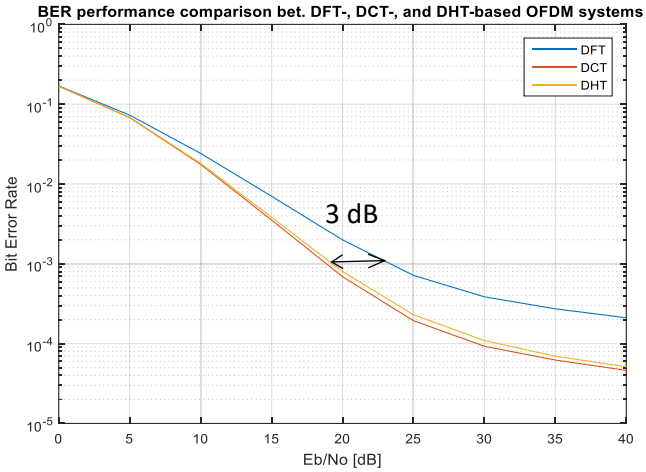

Figure 6: BER performance comparison between DFT-, DCT-, and DHT-based OFDM systems

7.2. CCDF Comparison of DFT-, DCT-, and DHT-based OFDM systems using SLM and PTS PAPR reduction techniques

The Selective Mapping (SLM) technique is an efficient way to reduce the Peak-to-Average Power Ratio (PAPR) in OFDM systems. The concordance of simulation results with theoretical predictions bolsters the reliability of the SLM technique in diverse OFDM systems, including those utilizing DFT, DCT, and DHT.

The continual reduction in PAPR across many systems underscores the adaptability and efficiency of the SLM methodology. This indicates that irrespective of the transformation employed in the OFDM system, SLM can yield substantial enhancements in PAPR, which is essential for improving the efficiency and performance of wireless communication systems.

Figure 7 illustrates the PAPR performance of various systems employing the SLM reduction technique. The results show that the reduction of different OFDM systems is approximately the same and needs around (4) dB to reach the corresponding CCDF (10^{-3}).

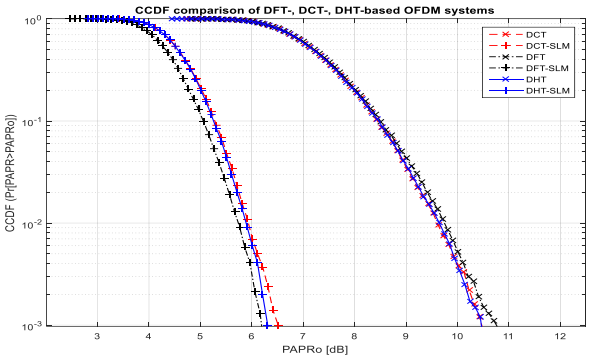

Figure 7: CCDF comparison of DFT-, DCT-, and DHT-based OFDM systems using SLM reduction technique.

PTS is regarded as one of the most effective PAPR reduction techniques due to its efficiency and low complexity. Figure 8 illustrates the PAPR performance of various systems employing the PTS reduction technique. The results show that the reduction of different OFDM systems is approximately the same and needs γ around (4) dB to reach the corresponding CCDF (10^{-3})

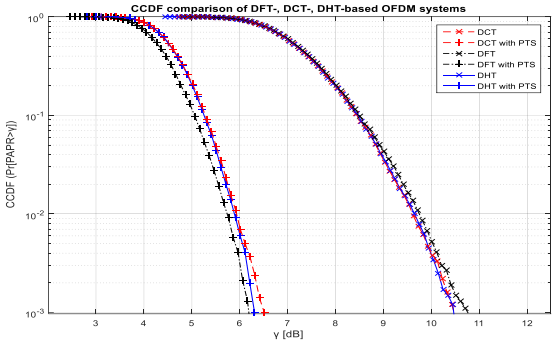

Figure 8: CCDF comparison of DFT-, DCT-, and DHT-based OFDM systems using PTS reduction technique.

8. Conclusion

This study employed DCT-based and DHT-based OFDM systems instead of the conventional DFT-based OFDM system across doubly dispersive fading channels with fluctuating Doppler shifts. Under constant operation conditions (without Doppler shift), the DFT-based OFDM system surpassed the DCT- and DHT-based systems. Nonetheless, the IEEE 802.11a standard indicated a deterioration in performance for the DFT-based OFDM system in mobile environments. The simulation results showed that the DFT-based OFDM system surpassed the DCT-based OFDM system in terms of BER. Moreover, the OFDM system utilizing DHT exhibited superior performance compared to the OFDM system employing DFT. The results indicated that in doubly dispersive fading conditions, the performance of DCT- and DHT-based OFDM systems was similar, exceeding that of the DFT-based OFDM system by approximately 3 dB in Signal-to-Noise Ratio. Furthermore, the CCDF comparison indicated that the PAPR reduction approaches (SLM or PTS) uniformly reduced PAPR by the same magnitude across all OFDM systems. This demonstrates that DCT- and DHT-based OFDM systems attain equivalent PAPR reduction while providing superior BER performance and diminished system complexity, owing to the utilization of real arithmetic, hence effectively lowering complexity and power consumption relative to DFT-based signal processing.

This research exclusively examines Single Input Single Output (SISO) OFDM systems. This can be expanded to MIMO OFDM, which can be executed utilizing multiple sending and receiving antennas, representing a compelling area for future research.

Conflict of Interest

The authors declare no conflict of interest.

References

[1] Mahmoud A. Abdelghany, Yehia S. Mohamed, and Asmaa R.Wardany, "Improved performance of LNA using high quality factor PGS on-chip spiral inductors," JAET on, vol. 38, pp. 161-171, 2019.

[2] Ashraf A. M. Khalaf, Mohamed Elnabawy, and Nazmi Azzam, "Non-linear companding techniques with aco-OFDM-based VLC systems for PAPR reduction," JAET on, vol. 42, pp. 53-69, 2023.

[3] Hrycak, Tomasz, and Gerald Matz. "Low-complexity time-domain ICI equalization for OFDM communications over rapidly varying channels." 2006 Fortieth Asilomar Conference on Signals, Systems and Computers. IEEE, 2006.

[4] Solyman, Ahmed AA, Stephan Weiss, and John J. Soraghan. "Low-complexity LSMR equalisation of FrFT-based multicarrier systems in doubly dispersive channels." 2011 IEEE international symposium on signal processing and information technology (ISSPIT). IEEE, 2011.

[5] Barhumi, Imad, Geert Leus, and Marc Moonen. "Equalization for OFDM over doubly selective channels." IEEE Transactions on Signal Processing 54.4 (2006): 1445-1458.

[6] Martone, Massimiliano. "A multicarrier system based on the fractional Fourier transform for time-frequency-selective channels." IEEE Transactions on Communications 49.6 (2001): 1011-1020.

[7] C. Chen, X. Zhong, M. Liu and H. Y. Fu, "DHT-OFDM Based Spatial Modulation for Optical Wireless Communication," 2020 IEEE 5th Optoelectronics Global Conference (OGC), Shenzhen, China, 2020, pp. 32-35,

[8] Sari, Hikmet, Georges Karam, and Isabelle Jeanclaude. "Transmission techniques for digital terrestrial TV broadcasting." IEEE communications magazine 33.2 (1995): 100-109.

[9] Alsisi, Rayan H., and Raveendra K. Rao. "DCT-and FFT-based OFDM systems with continuous phase modulation over flat fading channels." 2017 International Conference on Electrical and Computing Technologies and Applications (ICECTA). IEEE, 2017.

[10] Alsisi, Rayan H., and Raveendra K. Rao. "Performance of constant envelope DCT based OFDM system with M-ary PAM mapper in AWGN channel." 2017 Annual IEEE International Systems Conference (SysCon). IEEE, 2017.

[11] O'hara, Bob, and Al Petrick. IEEE 802.11 handbook: a designer's companion. IEEE Standards Association, 2005.

[12] Jao, Chin-Kuo, Syu-Siang Long, and Muh-Tian Shiue. "DHT-based OFDM system for passband transmission over frequency-selective channel." IEEE Signal Processing Letters 17.8 (2010): 699-702.

[13] Choi, Yang-Seok, Peter J. Voltz, and Frank A. Cassara. "On channel estimation and detection for multicarrier signals in fast and selective Rayleigh fading channels." IEEE Transactions on Communications 49.8 (2001): 1375-1387.

[14] Solyman, Ahmed AA, et al. "Hybrid FrFT and FFT based Multimode Transmission OFDM System Based." The International Conference on Electrical Engineering. Vol. 8. No. 8th International Conference on Electrical Engineering ICEENG 2012. Military Technical College, 2012.

[15] Robertson, Patrick, and Stefan Kaiser. "Analysis of the loss of orthogonality through Doppler spread in OFDM systems." Seamless Interconnection for Universal Services. Global Telecommunications Conference. GLOBECOM'99.(Cat. No. 99CH37042). Vol. 1. IEEE, 1999.

[16] Rugini, Luca, and Paolo Banelli. "Performance analysis of banded equalizers for OFDM systems in time-varying channels." 2007 IEEE 8th Workshop on Signal Processing Advances in Wireless Communications. IEEE, 2007.

[17] Jeon, Won Gi, Kyung Hi Chang, and Yong Soo Cho. "An equalization technique for orthogonal frequency-division multiplexing systems in time-variant multipath channels." IEEE transactions on communications 47.1 (1999): 27-32.